

1 **Variability in ice cover does not affect annual metabolism estimates in a small eutrophic**
2 **reservoir**

3
4 Dexter W. Howard¹, Jennifer A. Brentrup², David C. Richardson³, Abigail S. L. Lewis¹, Freya E.
5 Olsson¹, Cayelan C. Carey¹
6

7 ¹Department of Biological Sciences, Virginia Tech, Blacksburg, VA, USA

8 ²Minnesota Pollution Control Agency, Saint Paul, MN, USA

9 ³Biology Department, SUNY New Paltz, New Paltz, NY, USA

10
11 Corresponding author: Dexter W. Howard (dwh1998@vt.edu)

12
13 ORCIDs:

14 Dexter W. Howard: 0000-0002-6118-2149

15 Jennifer A. Brentrup: 0000-0002-4818-7762

16 David C. Richardson: 0000-0001-9374-9624

17 Abigail S. L. Lewis: 0000-0001-9933-4542

18 Freya E. Olsson: 0000-0002-0483-4489

19 Cayelan C. Carey: 0000-0001-8835-4476
20

21 CRediT taxonomy:

22 Conceptualization: DWH, CCC

23 Data curation: DWH, ASLL

24 Formal analysis: DWH

25 Funding acquisition: CCC

26 Investigation: DWH, JAB, DCR, ASLL, FEO, CCC

27 Methodology: DWH, JAB, DCR, ASLL, FEO, CCC

28 Project administration: DWH, CCC

29 Software: DWH, JAB, DCR

30 Supervision: CCC

31 Validation: FEO

32 Visualization: DWH, JAB, DCR

33 Writing - original draft: DWH

34 Writing - review and editing: DWH, JAB, DCR, ASLL, FEO, CCC
35

36 **Keywords:** ecosystem respiration (R), gross primary production (GPP), lake metabolism, net
37 ecosystem production (NEP), reservoirs, winter limnology
38

39 **Key Points:**

- 40
- 41 ● Winter data have rarely been included in lake metabolism studies, limiting our
42 understanding of how ice affects metabolism estimates
 - 43 ● Annual metabolism estimates were similar across 6 years with widely varying ice cover
 - 44 ● Water chemistry explained variability in daily gross primary production, but not
45 respiration or net ecosystem production, over 6 years

46 **Abstract (250 words)**

47 Temperate reservoirs and lakes worldwide are experiencing decreases in ice cover,
48 which will likely alter the net balance of gross primary production (GPP) and respiration (R) in
49 these ecosystems. However, most metabolism studies to date have focused on summer
50 dynamics, thereby excluding winter dynamics from annual metabolism budgets. To address this
51 gap, we analyzed six years of year-round high-frequency dissolved oxygen data to estimate
52 daily rates of net ecosystem production (NEP), GPP, and R in a eutrophic, dimictic reservoir that
53 has intermittent ice cover. Over six years, the reservoir exhibited slight heterotrophy during both
54 summer and winter. We found winter and summer metabolism rates to be similar: summer NEP
55 had a median rate of $-0.06 \text{ mg O}_2 \text{ L}^{-1} \text{ day}^{-1}$ (range: -15.86 to $3.20 \text{ mg O}_2 \text{ L}^{-1} \text{ day}^{-1}$), while median
56 winter NEP was $-0.02 \text{ mg O}_2 \text{ L}^{-1} \text{ day}^{-1}$ (range: -8.19 to $0.53 \text{ mg O}_2 \text{ L}^{-1} \text{ day}^{-1}$). Despite large
57 differences in the duration of ice cover among years, there were minimal differences in NEP
58 among winters. Overall, the inclusion of winter data had a limited effect on annual metabolism
59 estimates, likely due to short winter periods in this reservoir (ice durations 0–35 days) relative to
60 higher-latitude lakes. Our work reveals a smaller difference between winter and summer NEP
61 than in lakes with continuous ice cover. Ultimately, our work underscores the importance of
62 studying full-year metabolism dynamics in a range of aquatic ecosystems to help anticipate the
63 effects of declining ice cover across lakes worldwide.

64

65 **Plain Language Summary (200 words):**

66 Lakes and reservoirs around the world are experiencing decreases in ice cover duration,
67 with many waterbodies starting to experience non-continuous ice cover throughout the winter.
68 These changes in ice duration have the potential to influence carbon cycling, but to date few
69 long-term studies have included winter data. We analyzed six years of minute-resolution oxygen
70 data from a small reservoir that experiences non-continuous ice cover to estimate whether the
71 surface water was a source or sink of carbon at daily, seasonal, and annual scales. We found

72 that the reservoir was often a source of carbon to the atmosphere, regardless of whether data
73 from winter were included. Our results differed from previous studies conducted in higher-
74 latitude lakes that experience continuous ice cover throughout the winter, potentially due to the
75 already-short duration of ice cover in this reservoir. As the duration of ice cover continues to
76 decrease across lakes and reservoirs worldwide, our work highlights the need for studying how
77 changing winter conditions – especially non-continuous ice cover – affects year-round carbon
78 cycling.

79

80 **1 Introduction**

81 Changing climate and the shrinking duration of winter are altering the role of freshwater
82 ecosystems in the global carbon cycle (IPCC, 2022), which can be quantified using functional
83 ecosystem metrics (Brentrup et al., 2021; North et al., 2023; Palmer & Richardson, 2009). One
84 commonly used functional metric is net ecosystem production (NEP), the balance of whole
85 ecosystem gross primary production (GPP) and respiration (R), which can elucidate whether
86 freshwaters are net sources or sinks of organic carbon. Negative NEP indicates heterotrophy,
87 whereas positive NEP indicates ecosystem autotrophy (Lovett et al., 2006). Studies quantifying
88 ecosystem metabolism rates (i.e., NEP, GPP, and R) have primarily focused on the metabolism
89 of naturally-formed lakes in the summer months (e.g., Richardson et al., 2017; Solomon et al.,
90 2013; but see Williamson et al., 2021), leaving substantial uncertainty as to how these rates
91 vary among seasons and years in the face of climate change. Multiple studies in north
92 temperate lakes have shown that winter metabolism rates are more heterotrophic than summer
93 rates (Brentrup et al., 2021; North et al., 2023; Rabaey et al., 2021), and that the inclusion of
94 winter rates in annual estimates can shift lakes from autotrophic to heterotrophic (Brentrup et
95 al., 2021), highlighting the importance of monitoring lake and reservoir metabolism year-round.

96 Lakes and reservoirs can be net autotrophic or heterotrophic (Hanson et al., 2003;
97 Hoellein et al., 2013), with shifts between autotrophy and heterotrophy occurring throughout the
98 year (Brentrup et al., 2021; Rabaey et al., 2021). Some north temperate lakes with trophic
99 states ranging from eutrophic to oligotrophic have been found to be autotrophic in summers but
100 heterotrophic in winters (Brentrup et al., 2021; North et al., 2023; Rabaey et al., 2021), while
101 other lakes in subtropical regions are autotrophic in both summer and winter (Hu et al., 2015).
102 While these few studies demonstrate that intra-annual variation in metabolism can occur in at
103 least some lakes, there is still much uncertainty in the prevalence, magnitude, and drivers of
104 intra-annual variation in metabolism in freshwater ecosystems. Understanding intra-annual
105 variation is important as previous work has found that inferring annual NEP from summer-only
106 measurements can result in biased metabolism rates (Brentrup et al., 2021). Additionally,
107 annual metabolism estimates can vary substantially year to year (Pace et al., 2021; Richardson
108 et al., 2017), supporting the need for multi-year metabolism studies to better understand how
109 NEP changes both within and among years.

110 Previous studies have shown that the environmental drivers of metabolism in naturally-
111 formed lakes during the open-water period vary across lakes (Solomon et al., 2013), within
112 years (Hu et al., 2015; Brentrup et al., 2021), and among years (Oleksy et al., 2022; Richardson
113 et al., 2017), but less is known about the drivers of metabolism in human-made reservoirs. For
114 example, nutrient concentrations have been positively correlated with GPP and R across lakes
115 (Solomon et al., 2013) and between years (Richardson et al., 2017), whereas local meteorology
116 (Hu et al., 2015; Richardson et al., 2017), hydrology (Klug et al., 2012), and water temperature
117 (Hu et al., 2015) have been found to be important drivers of intra-annual variation in
118 metabolism. These important advances in our understanding of metabolism in naturally-formed
119 lakes during the open-water period (Hanson et al., 2003; Hu et al., 2015; Richardson et al.,
120 2017; Solomon et al., 2013) set the stage for increasing our understanding of the drivers of
121 year-round metabolism dynamics in human-made reservoirs, which are understudied relative to

122 naturally-found lakes (Doubek & Carey, 2017). In reservoirs, which have shorter residence
123 times and greater catchment to lake area ratios than naturally-formed lakes (Hayes et al., 2017),
124 we expect hydrology to be an important driver of metabolism (Oleksy et al., 2022; Williamson et
125 al., 2021), as shorter residence times will lead to more rapid turnover of nutrients and organic
126 carbon that can stimulate R and GPP (Catalán et al., 2016; Hanson et al., 2003).

127 The presence of ice can affect winter metabolism estimates in lakes and reservoirs in
128 contradictory ways, by either stimulating or repressing phytoplankton growth (Jewson et al.,
129 2009). In some cases, similar or even higher levels of phytoplankton biomass can persist under-
130 ice when compared to open-water, resulting in increased GPP (Hampton et al., 2017; Jewson et
131 al., 2009; Twiss et al., 2012). However, under other conditions (e.g., opaque ice or snow cover),
132 phytoplankton productivity may be limited, decreasing winter GPP and resulting in net
133 heterotrophy (Jewson et al., 2009; Leppäranta et al., 2012; North et al., 2023). These variable
134 responses highlight the need for characterizing under-ice metabolism as ice cover and
135 thickness is decreasing on lakes worldwide (Magnuson et al., 2000; Sharma et al., 2021;
136 Weyhenmeyer et al., 2022). However, estimating under-ice metabolism rates remains a major
137 challenge due to the logistical difficulties of winter data collection, especially in sites with
138 intermittent ice that prevent safe conditions to sample and deploy sensors (Block et al., 2019).
139 As a result, most winter metabolism studies have been conducted in naturally-formed lakes that
140 experience continuous ice cover throughout the winter (e.g., Brentrup et al., 2021; Huang et al.,
141 2021; Obertegger et al., 2017; Song et al., 2019). Consequently, research on intermittently ice-
142 covered freshwater ecosystems is needed to improve our understanding of the role dynamic ice
143 cover plays on annual metabolism rates as climate change increases the prevalence of winters
144 in which north temperate waterbodies experience intermittent or even no ice cover (Sharma et
145 al., 2019).

146 To improve our understanding of intra-annual and inter-annual variability in freshwater
147 metabolism, we estimated six years of daily rates of GPP, R, and NEP using inverse modeling

148 of high-frequency dissolved oxygen (DO) data in a eutrophic reservoir with variable and
149 intermittent ice cover. These six years of data represent the longest continuous record of
150 metabolism calculated from inverse modeling of high-frequency DO data, to the best of our
151 knowledge. We used these metabolism estimates to answer: 1) What is the inter- and intra-
152 annual variability of metabolism in a dimictic reservoir that exhibits intermittent ice conditions in
153 winter? 2) How do estimates of winter metabolism affect annual metabolism estimates? and 3)
154 What are the most important drivers of variability in metabolism? We first predicted higher R and
155 lower GPP estimates in winter (vs. summer) months. Second, we expected that the inclusion of
156 winter metabolism rates, especially in winters with extended ice cover duration, would lead to
157 higher annual R estimates and shift annual NEP towards heterotrophy, compared to winters
158 with a shorter duration of ice cover. Finally, we expected that the magnitude of reservoir GPP
159 and R estimates would be positively correlated with nutrient and carbon concentrations and with
160 reservoir inflow rates.

161

162 **2 Methods**

163 *2.1 Analysis Overview*

164 To quantify the magnitude and drivers of intra- and inter-annual metabolism in a
165 eutrophic reservoir, we modeled GPP, R, and NEP using high-frequency observational data,
166 then used time series analysis to identify drivers of the metabolic rates at multiple time scales.
167 First, we monitored DO and multiple environmental variables over the six-year monitoring period
168 (Section 2.3). Second, we used an inverse model (Section 2.4) with inputs of high-frequency
169 DO, water temperature at multiple depths, photosynthetically active radiation (PAR), and wind
170 speed (Section 2.3.1) to estimate GPP and R, from which we calculated NEP. Third, we
171 classified seasons using multiple approaches to compare metabolism at different times of year
172 (Section 2.3.3, Section 2.5.2). Fourth, we quantified metabolism variability, differences in

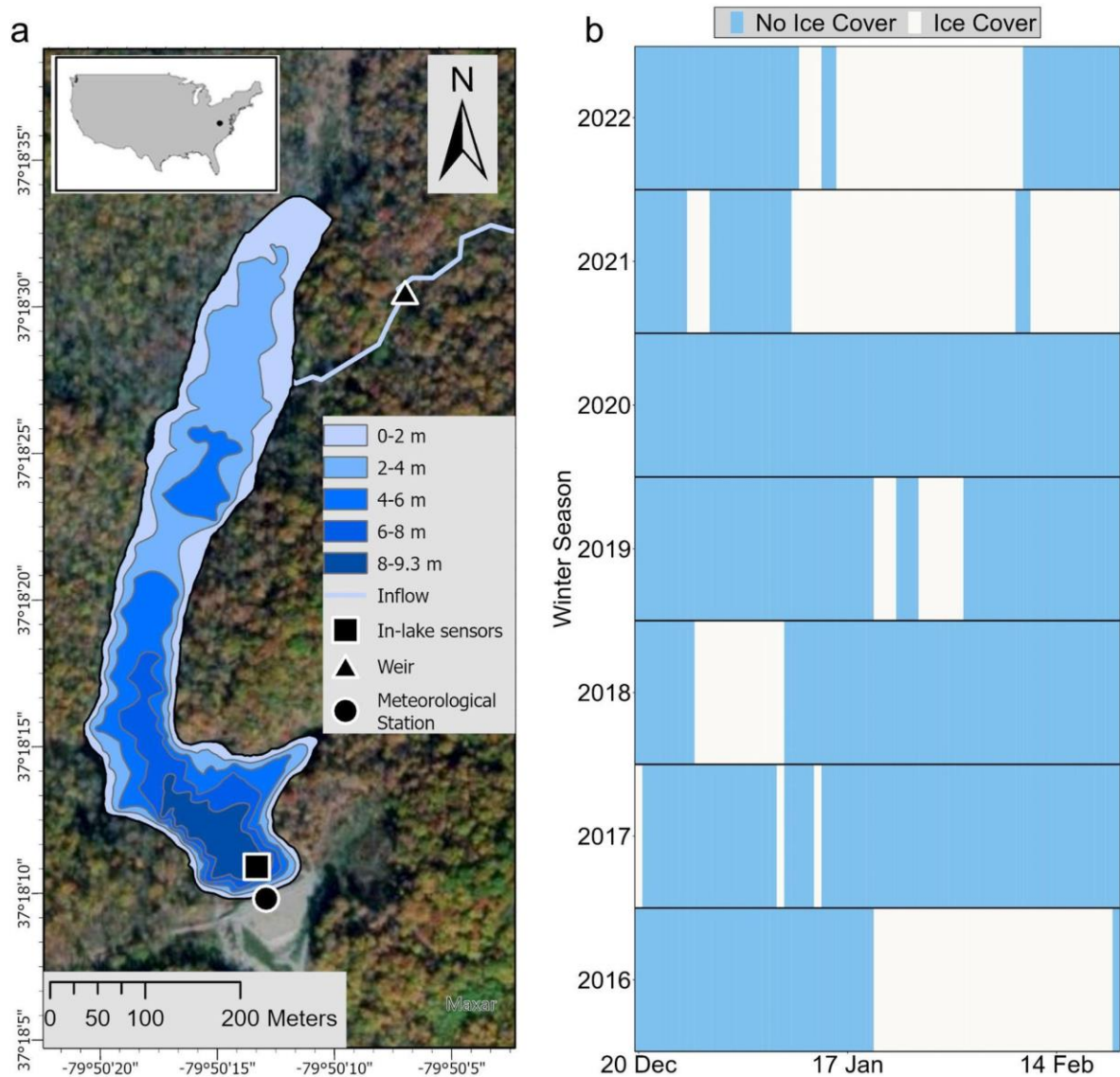
173 metabolism among seasons and years, and the importance of environmental drivers, including
174 meteorology, water chemistry, and hydrology, on reservoir metabolism (Section 2.5).

175

176 *2.2 Study Site*

177 Falling Creek Reservoir (FCR) is a small eutrophic reservoir located in Vinton, Virginia,
178 USA (37.30°N, 79.84°W; Figure 1a). FCR has a surface area of 0.12 km², a maximum depth of
179 9.3 m, a mean depth of 4 m, and a catchment to surface area ratio of 29:1 (Gerling et al., 2014;
180 Howard et al., 2021). FCR is a drinking water source located in a primarily deciduous forested
181 catchment and is owned and managed by the Western Virginia Water Authority. FCR is typically
182 dimictic with summer thermal stratification usually occurring between March and October and
183 intermittent ice cover between December and February (Carey & Breef-Pilz, 2022; Figure 1b).
184 Throughout the monitoring period of 9 November 2015 – 28 February 2022, the water level in
185 FCR was managed to be at full capacity, with only small fluctuations. Water residence time
186 during the duration of the study had a median of 185 days (interquartile range of 56 – 512 days),
187 following the calculation methods of Gerling et al. (2014). The reservoir is fed by one primary
188 inflow, which contributes ~95% of the water budget (Gerling et al., 2016).

189



190
 191 *Figure 1. a) Map of Falling Creek Reservoir (FCR) and its primary inflow stream, located in*
 192 *Vinton, Virginia, USA. The inset map depicts the location of the reservoir within the coterminous*
 193 *USA. b) Time series of ice cover duration in FCR in each winter season (operationally defined*
 194 *as 20 December – 22 February, Section 2.5.2). White shading denotes ice cover and light blue*
 195 *shading denotes ice-free (open-water) periods.*

196 *2.3 Field Data Collection*

197 *2.3.1 High-Frequency Sensor Data Collection*

198 A high-frequency optical DO sensor was deployed in the epilimnion at the deepest site in
199 FCR to capture diel DO dynamics over the 2015–2022 monitoring period (Figure 1). From 9
200 November 2015 to 31 December 2018, an InsiteIG Model20 DO sensor (Insite Instrumentation
201 Group, Slidell, LA, USA) measured DO concentration and water temperature every 15 minutes
202 at 1 m below the surface (Carey, Howard, Gantzer, et al., 2023). From 29 August 2018 to 28
203 February 2022, a YSI EXO2 sonde (YSI Incorporated, Yellow Springs, OH, USA) measured DO
204 and water temperature every ten minutes at 1.6 m below the surface (Carey, Breef-Pilz, &
205 Woelmer, 2023). The EXO2 was deployed at 1.6 m to correspond with a water outtake valve
206 and was additionally equipped with chlorophyll-*a* and fluorescent dissolved organic matter
207 sensors (Carey, Breef-Pilz, & Woelmer, 2023). To harmonize the DO data between the two
208 sensors and calculate metabolism over a near-continuous period from 9 November 2015 to 28
209 February 2022, we compared the five-month long period when both sensors were
210 simultaneously deployed (August 2018 to January 2019), and applied a linear offset to the 1-m
211 InsiteIG sensor data from the 1.6-m YSI DO sensor based off the median difference between
212 sensor observations (see Supplementary Text S1 and Supplementary Figure S1 for details).

213 Water temperature profiles were collected at the deepest site of FCR with a suite of
214 sensors during the monitoring period. From 9 November 2015 to 14 January 2018, a depth
215 profile of water temperature was measured at 1-m intervals from 1 m below the surface to just
216 above the sediments (9 m) every 10 to 15 minutes using HOBO thermistors (HOBO Pendant
217 Temperature Data Logger, Bourne, MA, USA; Carey, Howard, Gantzer, et al., 2023). In July
218 2018, NexSens T-Node FR Thermistors (Fondriest Environmental Inc., Fairborn, OH, USA)
219 were deployed at the same site at FCR and also monitored water temperature at 1-m intervals
220 from the surface to the bottom of FCR every 10 minutes (Carey, Breef-Pilz, & Woelmer, 2023).
221 We applied standardized gap-filling procedures to fill the continuous five months of missing

222 values when no thermistors were deployed by using modeled temperature profiles (Carey,
223 Hanson, et al., 2022) and interpolated manual weekly profiles (see Supplementary Text S2).

224 A research-grade meteorological station (Campbell Scientific, Logan, UT, USA) was
225 deployed on FCR's dam throughout the monitoring period (Figure 1) to collect one-minute
226 resolution downwelling shortwave radiation, precipitation, air temperature, and wind speed
227 measurements (see Carey & Breef-Pilz, 2023a for sensor specifications). We calculated PAR
228 from downwelling shortwave radiation using the R *LakeMetabolizer* package (Winslow et al.,
229 2016). PAR and wind speed data were averaged to 10 or 15-minute resolution to match
230 dissolved oxygen data used in the metabolism model (Section 2.4). Meteorological data had
231 three gaps due to sensor maintenance ranging in duration from 16 to 77 days. We filled these
232 gaps using regressions developed between observed meteorology and data from the North
233 American Land Data Assimilation System-2 (NLDAS-2; Xia et al., 2012; Supplementary Text
234 S2, Supplementary Figures S2 and S3). Reservoir inflow discharge was calculated every fifteen
235 minutes from the primary tributary to FCR (Figure 1) at a weir equipped with an INW Aquistar
236 PT2X pressure sensor (INW, Kirkland, WA; see Carey & Breef-Pilz, 2023b for details).

237

238 *2.3.2 Weekly Environmental Driver Sampling*

239 In addition to high-frequency sensors, we collected weekly to monthly measurements of
240 light and water chemistry to determine drivers of metabolism variability. Light attenuation was
241 estimated using light extinction coefficients (K_d) from vertical PAR profiles collected at the
242 deepest site of the reservoir using either a conductivity, temperature, and depth (CTD) profiler
243 (SBE 19 plus CTD profiler, Seabird Electronics, Bellevue, WA, USA) or handheld PAR sensor
244 (LiCor LI-192 underwater quantum sensor, LI-COR Biosciences, Lincoln, NE, USA) weekly from
245 spring to fall and monthly through the winter (Carey, Lewis, & Breef-Pilz, 2023). When sensor
246 data were not available, light attenuation was estimated from Secchi disk measurements at a
247 weekly frequency from spring to fall and monthly through the winter (Carey, Breef-Pilz, Wander,

248 et al., 2023). Light attenuation measured via the Secchi and PAR sensor profile methods gave
249 similar K_d estimates (median K_d from sensors = 1.0 m^{-1} ; median K_d from Secchi = 1.1 m^{-1}). We
250 additionally calculated the derived mean daily mixed layer irradiance (\bar{E}_{24}), a measure of mean
251 light experienced by phytoplankton, from K_d , mixed layer depth, and daily incident irradiance
252 data (\bar{E}_0 ; Guildford et al., 2000; Pernica et al., 2017).

253 Throughout the monitoring period, we collected weekly (spring to fall) to monthly (winter)
254 water samples at 1.6 m for dissolved organic carbon (DOC), nitrogen (total nitrogen (N), nitrate,
255 and ammonium), and phosphorus (total phosphorus (P) and soluble reactive P). All N and P
256 samples were analyzed colorimetrically using flow injection analysis on a Lachat Instruments
257 XYZ Autosampler ASX 520 Series and QuikChem Series 8500 (Lachat ASX 520 Series, Lachat
258 Instruments, Loveland, Colorado, USA; Carey, Wander, Howard, et al., 2023). DOC was
259 analyzed using the persulfate catalytic method on a Total Organic Carbon Analyzer (TOCA)
260 from OI Analytical from 2015-2016 (OI Analytical 1010 TOCA with 1051 autosampler, College
261 Station, TX USA) and on a Vario TOC Cube from Elementar from 2016-2022 (vario TOC cube,
262 Elementar Analysensysteme GmbH, Hanau, Germany; Carey, Wander, Howard, et al., 2023).

263

264 2.3.3 Ice cover monitoring

265 Ice cover at FCR was classified as the presence of ice covering greater than 50% of the
266 deep hole basin of the reservoir (Figure 1), regardless of ice thickness, and was determined
267 using three methods (Carey & Breef-Pilz, 2022). First, the presence of ice was assessed by
268 visual observation from observers standing at the deep hole of the reservoir or from automated
269 cameras (Carey & Breef-Pilz, 2022). If visual observations were not available, we next checked
270 for the presence of inverse stratification via water temperature profiles, which was validated by
271 looking for changes in upwelling shortwave radiation and albedo from the reservoir (Carey &
272 Breef-Pilz, 2022). Finally, we looked for the depletion of DO at 9 m depth in FCR, using an
273 InSitu RDO Pro-X Dissolved Oxygen Sensor (In-Situ Inc., Fort Collins, CO, USA) deployed at

274 the same site as the epilimnetic DO sondes (Carey, Breef-Pilz, & Woelmer, 2023). This sensor
275 collected DO measurements every ten minutes and was used to monitor for winter DO
276 depletion, as hypolimnetic DO depletion is noticeable when ice cover duration exceeds one day
277 (Carey & Breef-Pilz, 2022).

278

279 *2.4 Metabolism model*

280 Daily estimates of GPP and R were calculated using an open-water inverse modeling
281 method that can account for under-ice and open-water periods (Hanson et al., 2008, as
282 implemented by Brentrup et al., 2021). Model input data included epilimnetic DO concentrations,
283 epilimnetic water temperature, water temperature profiles, wind speed at 10 m, and PAR. The
284 open water model is based on Equation 1 (Hanson et al., 2008; Odum, 1956), in which changes
285 in dissolved oxygen concentration (dDO/dt) are calculated as:

$$286 \quad \frac{dDO}{dt} = GPP - R + D \text{ (eqn. 1)}$$

287 where D is atmospheric oxygen flux.

288 DO dynamics were then modeled every 10 – 15 minutes (depending on sensor
289 frequency) following Equation 2 (Richardson et al., 2017; Solomon et al., 2013; Van de Bogert
290 et al., 2007):

$$DO_{t+1} = DO_t + g \times I_t - r + D_t + \gamma_t \text{ (eqn. 2)}$$

291 Where DO_t and DO_{t+1} represent DO concentrations at times t and $t+1$; g is the parameter
292 describing the rate of photosynthesis per I_t ; I_t is incoming PAR at time t ; r is the parameter
293 describing a mean rate of respiration; D_t is atmospheric flux of oxygen; and γ_t represents
294 process error.

295 Atmospheric flux of DO was modeled every 10 – 15 minutes following Equation 3
296 (Richardson et al., 2017; Solomon et al., 2013):

$$D_t = d_t \times (-k_t) \times (DO_t - S_t) / z_t \text{ (eqn. 3)}$$

297 Where k_t is the piston velocity of oxygen calculated using wind speed every ten minutes (Cole &
298 Caraco, 1998); S_t is the saturation concentration of DO based on water temperature and
299 atmospheric pressure; z_t is the mixed layer depth calculated based on the water density
300 gradient using water temperature profiles following Coloso et al. (2011); and d_t is a binary
301 variable used to represent if the DO sonde was above or below z_t . A d_t of 1 indicates the DO
302 sonde is above z_t and oxygen can exchange with the atmosphere, vs. a d_t of 0 indicates the
303 sonde is below z_t and oxygen cannot exchange with the atmosphere. Atmospheric flux was
304 assumed to be zero during periods of ice cover following Brentrup et al. (2021).

305 GPP and R were modeled as parameters through the optimization of the metabolism
306 model in Equation 2 using a Nelder-Mead optimization algorithm that reduces the negative log-
307 likelihood of the error (γ_t) in Equation 2, following Solomon et al. (2013) and Richardson et al.
308 (2017), and based on Hanson et al. (2008) and Van de Bogert et al. (2007). GPP and R were
309 then scaled from 10 – 15 minute rates to daily rates of GPP and R reported in $\text{mg O}_2 \text{L}^{-1} \text{day}^{-1}$
310 (Richardson et al., 2017).

311

312 *2.5 Statistical analyses*

313 *2.5.1 Q1: What is the inter- and intra-annual variability of metabolism in a dimictic reservoir?*

314 To investigate inter-annual and intra-annual variation in metabolism rates, we compared
315 metabolism between open-water and under-ice periods within the winter, among seasons in the
316 year, and across years. We were able to fit estimates of GPP and R for 54% of the $n = 2302$
317 total days in our time series when GPP and R were above ecologically meaningful rates of
318 $0.001 \text{ mg O}_2 \text{L}^{-1} \text{day}^{-1}$ (following Brentrup et al., 2021); values below those rates were set as NA.
319 Our proportion of model fits was similar to another study with one year of data that compared
320 under-ice and open-water metabolism (57% days acceptable fits; Brentrup et al., 2021). NEP
321 was calculated for days with acceptable estimates of both GPP and R. Kruskal-Wallis rank sum
322 tests were used to test for significant differences in mean GPP, R, and NEP rates across years

323 and seasons (Hollander & Wolfe, 1973) using the *stats* package in R (R Core Team, 2023).

324 We compared intra and inter-annual variability by calculating the coefficient of variation
325 (CV) for GPP, R, and NEP for the entire time series, across groups of seasons, for individual
326 seasons, and for individual years. We applied the Levene's test to check for statistical
327 differences among GPP, R, and NEP using the *car* package in R (Fox & Weisberg, 2019).

328

329 *2.5.2 Q2: How do estimates of winter metabolism affect annual metabolism estimates?*

330 There are many different ways to classify seasons in lakes and reservoirs (e.g., Gray et
331 al., 2020; Jane et al., 2023; Pierson et al., 2011; Rabaey et al., 2021; Woolway et al., 2022);
332 here, we focus on results generated using operational definitions for each season. We tested
333 multiple seasonal classifications in our analysis, including the use of seasons defined by solar
334 equinoxes/solstices and thermal stratification periods, and note that alternate season
335 calculations did not affect our primary findings (Supplementary Text S3, Table S1, Figure S4). In
336 our operational definition of winter in FCR, winter was the period starting on the earliest date of
337 ice cover recorded across all years of our study (20 December, observed in 2016, Figure 1b)
338 and ending on the latest day of ice cover recorded across all years of our study (22 February,
339 observed in 2021, Figure 1b). Winter seasons were then classified as the duration from 20
340 December of the previous calendar year through 22 February of a given year (e.g., Winter 2020
341 was classified as 20 December 2019 – 22 February 2020). This operational definition of winter
342 was adapted from other studies studying lakes with continuous ice cover (Hampton et al., 2017;
343 Pierson et al., 2011; Woolway et al., 2022).

344 Similar to winter, summer was defined as the period starting on the earliest first day of
345 continuous summer thermal stratification recorded in any year of our study (9 March, observed
346 in 2016) and ending on the latest day of summer stratification recorded in any year of our study
347 (2 November, observed in 2021). This definition was chosen to correspond with other studies
348 that operationally classify summer as the period of continuous thermal stratification (Jane et al.,

2023; Ladwig et al., 2022). We used two metrics to determine the onset and end of summer stratification—both criteria had to be met for us to consider the reservoir stratified on a given date. First, we assessed whether the difference in water density between epilimnetic (1 m below the surface) and hypolimnetic (1 m above the sediments) water was at least 0.1 kg m^{-3} (Woolway et al., 2021). Density is a robust and widespread metric of stratification, with multiple studies using 0.1 kg m^{-3} as a threshold to determine the presence of stratification (e.g., Andersen et al., 2017; Ladwig et al., 2021; Woolway et al., 2021). Second, we analyzed whether Schmidt stability was greater than 2% of the summer maximum stability. Schmidt stability is a common metric for determining the strength of stratification in lakes (Duka et al., 2021; Sahoo et al., 2016) and was calculated using the *rLakeAnalyzer* R package (Winslow et al., 2019) according to Idso (1973) using water temperature profiles and bathymetry of FCR (Carey, Lewis, et al., 2022). Calculating the percent of maximum Schmidt stability enables comparison to other lakes or reservoirs. Together, we defined summer stratification as beginning on the first day that both criteria were met for the subsequent two weeks, to remove spring and fall days when stratification was setting up or intermittent. Following this definition, summer stratification ended on the first day when the density difference was less than or equal to 0.1 kg m^{-3} and percent maximum Schmidt stability was less than 2%.

The spring mixed period occurred between the first day after winter ended (23 February) and the day before onset of summer stratification (8 March), and fall was considered the period between the day after the end of summer stratification (3 November) and the day before winter began (19 December). Altogether, we defined a lake-year to span from 20 December of the prior calendar year to 19 December of a given year to prevent the transition between years occurring mid-winter and breaking up ecologically-relevant within-season dynamics (i.e., the 2016 lake-year was 20 December 2015 – 19 December 2016).

We conducted non-paired Wilcoxon tests to compare ice-covered and ice-free periods during the winter and Kruskal-Wallis tests to compare across seasons using the *stats* package

375 in R (R Core Team, 2023). Dunn post-hoc tests were used to determine statistical differences
376 between seasonal means when Kruskal-Wallis results were significant using the *FSA* package
377 in R (Ogle et al., 2023). To test the effect of including winter metabolism rates on annual
378 estimates, we used a paired t-test comparing annual estimates of NEP that included and
379 excluded winter rates.

380

381 2.5.3 Q3: What are the most important drivers of variability in metabolism?

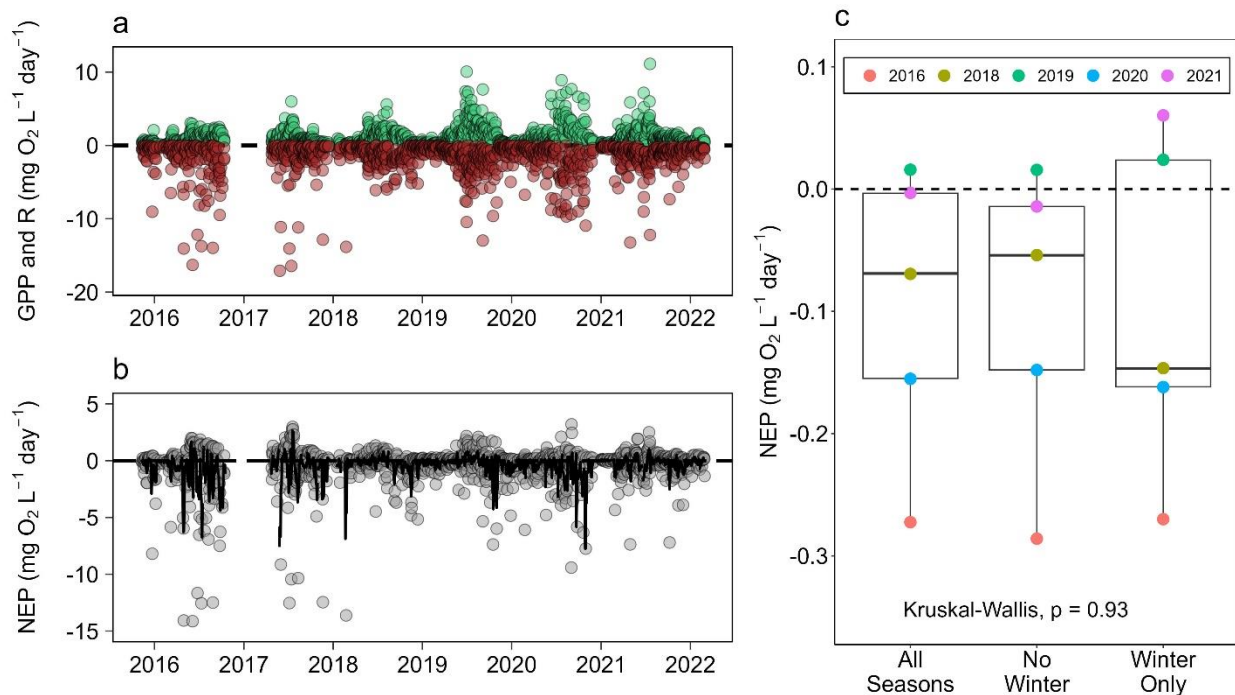
382 To identify environmental drivers of metabolism, we developed autoregressive (AR)
383 models for GPP, R, and NEP at daily timesteps. We collated daily data for air temperature,
384 precipitation, fluorescent dissolved organic matter, chlorophyll-a, reservoir inflow discharge, TN,
385 nitrate, ammonium, TP, SRP, DOC, Schmidt stability, K_d , and \bar{E}_{24} . We then developed
386 correlation matrices to identify collinearity between potential environmental driver variables,
387 defined as when two variables had a Spearman rank correlation of $r > 0.5$. For variables that
388 had $r > 0.5$, we tested which of the correlated variables had a stronger correlation to the
389 metabolism variable of interest based on univariate scatterplots and retained only the variable
390 with a stronger correlation (following McClure et al., 2020).

391 After removing collinear variables, there were seven candidate variables for daily models
392 of NEP (precipitation, TP, DOC, SRP, nitrate, ammonium, \bar{E}_{24}), GPP (precipitation, TP, TN,
393 SRP, nitrate, ammonium, \bar{E}_{24}), and R (precipitation, TP, DOC, SRP, nitrate, ammonium, \bar{E}_{24}).
394 We z-transformed predictors to enable comparison of the magnitude of coefficients in AR
395 models. We then developed global models for each metabolism metric that included an AR1 lag
396 term to account for temporal autocorrelation (Box & Pierce, 1970) and all possible combinations
397 of the non-collinear predictor variables, and ranked models by AICc to determine which models
398 best predicted metabolism rates using the *dredge* function in the *MuMIn* package in R (Bartoń,
399 2022). All analyses were conducted in R version 4.2.3 (R Core Team, 2023), with all code
400 archived in a Zenodo repository (Howard et al., 2024).

401 3 Results

402 3.1 Q1: What is the inter- and intra-annual variability of metabolism in a dimictic reservoir?

403 The magnitude and variability in R, GPP, and NEP differed among variables when
404 aggregated over the six-year study (Figure 2). The absolute value of R was greater than GPP
405 (Table 1), with a median R of $-0.99 \text{ mg O}_2 \text{ L}^{-1} \text{ day}^{-1}$ compared to $0.82 \text{ mg O}_2 \text{ L}^{-1} \text{ day}^{-1}$ (Wilcoxon
406 test $p < 0.001$). R was more variable than GPP (daily CVs of -1.29 and 1.05 , respectively;
407 Levene's test $p < 0.001$). NEP was near-zero or slightly negative in FCR (54% of days had
408 negative NEP when NEP could be estimated, $n = 1243$), with a median daily rate of -0.05 ± 1.79
409 $\text{mg O}_2 \text{ L}^{-1} \text{ day}^{-1}$ (Figure 2; Table 1), indicating that FCR was net heterotrophic across the study
410 period. NEP was more variable than R throughout the study period (CV = -3.85 ; Levene's test p
411 < 0.001) but was not more variable than GPP ($p = 0.08$).



412 Figure 2. a) Daily estimates of GPP (green points), R (brown points) in FCR from November
413 2015 through February 2022. b) Daily estimates of NEP (gray points) and seven-day moving
414 average of NEP (black line). c) Boxplots comparing annual median NEP calculated from daily
415 estimates from all seasons; only spring, summer, and autumn (excluding winter); and only
416 winter. The color of the points denotes different years. Metabolism estimates are not included
417 for 2017 due to missing DO data.
418

Table 1. Summary table of daily GPP, R, and NEP ($\text{mg O}_2 \text{L}^{-1} \text{day}^{-1}$) aggregated throughout our study period. Values are medians \pm 1 standard deviation for their respective study period. Columns denote different time periods. Ice-on and ice-off are a subset of the winter season. Seasons are operationally defined based on summer stratification and ice cover, as detailed in the Methods.

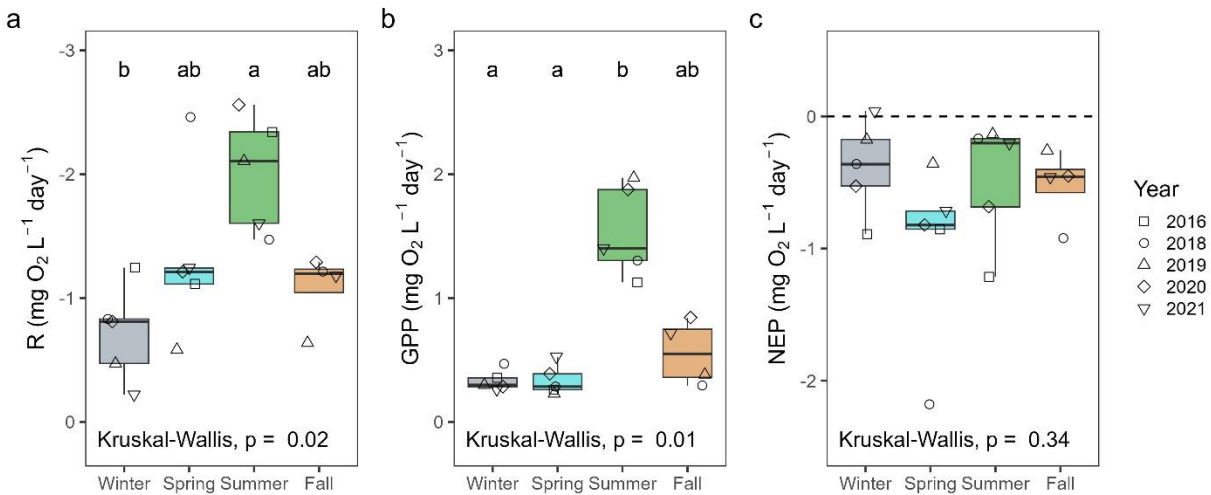
| Metabolism Rate | Full Time Series | Spring | Summer | Fall | Winter | | |
|---|------------------|------------------|------------------|------------------|------------------|------------------|------------------|
| | | | | | All | Ice-on | Ice-off |
| NEP ($\text{mg O}_2 \text{L}^{-1} \text{day}^{-1}$) | -0.05 \pm 1.79 | -0.08 \pm 2.45 | -0.06 \pm 1.89 | -0.03 \pm 1.49 | -0.02 \pm 0.96 | 0.03 \pm 0.29 | -0.09 \pm 1.07 |
| GPP ($\text{mg O}_2 \text{L}^{-1} \text{day}^{-1}$) | 0.82 \pm 1.27 | 0.34 \pm 0.22 | 1.15 \pm 1.35 | 0.38 \pm 0.34 | 0.26 \pm 0.31 | 0.22 \pm 0.42 | 0.27 \pm 0.26 |
| R ($\text{mg O}_2 \text{L}^{-1} \text{day}^{-1}$) | -0.99 \pm 2.15 | -0.46 \pm 2.45 | -1.26 \pm 2.28 | -0.51 \pm 1.49 | -0.36 \pm 1.01 | -0.21 \pm 0.48 | -0.40 \pm 1.11 |

419

420 FCR exhibited greater inter-annual variation in NEP than GPP and R throughout our
 421 study period (Figure 2). Across the five years with full data (i.e., 2015, 2017, and 2022 were
 422 excluded because they lacked estimates for all seasons), median annual NEP estimates ranged
 423 from $-0.27 \text{ mg O}_2 \text{L}^{-1} \text{day}^{-1}$ (in 2016) to $0.02 \text{ mg O}_2 \text{L}^{-1} \text{day}^{-1}$ (in 2019), and were statistically
 424 different across years (Kruskal-Wallis $H_4 = 16.7$, $p = 0.002$; Supplementary Figure S5,
 425 Supplementary Table S2). Median annual GPP and R were not as variable as NEP across
 426 years (Supplementary Figure S5), with GPP ranging from 0.80 to 0.95 $\text{mg O}_2 \text{L}^{-1} \text{day}^{-1}$ and R
 427 ranging from -0.96 to $-1.16 \text{ mg O}_2 \text{L}^{-1} \text{day}^{-1}$ (Supplementary Table S2). Neither GPP nor R were
 428 statistically different among years ($p = 0.22$ and $p = 0.16$, respectively). Variation in CV in
 429 distinct years also differed among metabolism rates, with annual NEP rates having the largest
 430 CV range (-6.63 to -2.40), while annual R and GPP rates had similar ranges of annual CV (-1.06
 431 to -1.41 and 0.73 to 1.12 , respectively; Supplementary Table S2).

432 While NEP was highly variable between years (Supplementary Figure S5), GPP and R
 433 exhibited higher variation across seasons (Figure 3), with median annual GPP and R estimates
 434 significantly different across seasons (Kruskal-Wallis $H_3 = 12.1$, $p < 0.01$; and $H_3 = 9.9$, $p < 0.02$;

435 respectively; Figure 3a, 3b). GPP and R were greater in the summer than other seasons when
 436 aggregated across years (Table 1, Figure 3a, 3b). Winter had the lowest median annual rates of
 437 GPP and R among seasons (Table 1). NEP was not significantly different between seasons
 438 (Kruskal-Wallis $H_3 = 3.3$, $p = 0.34$; Table 1; Figure 3c).



439

440 Figure 3. a, b, and c) Boxplots comparing median daily R, GPP, and NEP estimates across
 441 seasons per year. 2015, 2017, and 2022 were not included since they did not have estimates
 442 for multiple seasons.

443

444

Altogether, seasonal differences in median GPP were nearly six times higher than inter-
 445 annual differences (seasonal and inter-annual ranges = 0.89 and 0.15 $\text{mg O}_2 \text{L}^{-1} \text{day}^{-1}$,
 446 respectively; Table 1 and Supplementary Table S2), and four times higher in median R
 447 (seasonal and inter-annual ranges = 0.91 and 0.20 $\text{mg O}_2 \text{L}^{-1} \text{day}^{-1}$, respectively; Table 1 and
 448 Supplementary Table S2). In contrast, median NEP seasonal differences were nearly five times
 449 less than inter-annual variation (seasonal and inter-annual ranges = 0.06 and 0.29 $\text{mg O}_2 \text{L}^{-1}$
 450 day^{-1} , respectively; Table 1 and Supplementary Table S2).

451

452 3.2 Q2: How do estimates of winter metabolism affect annual metabolism estimates?

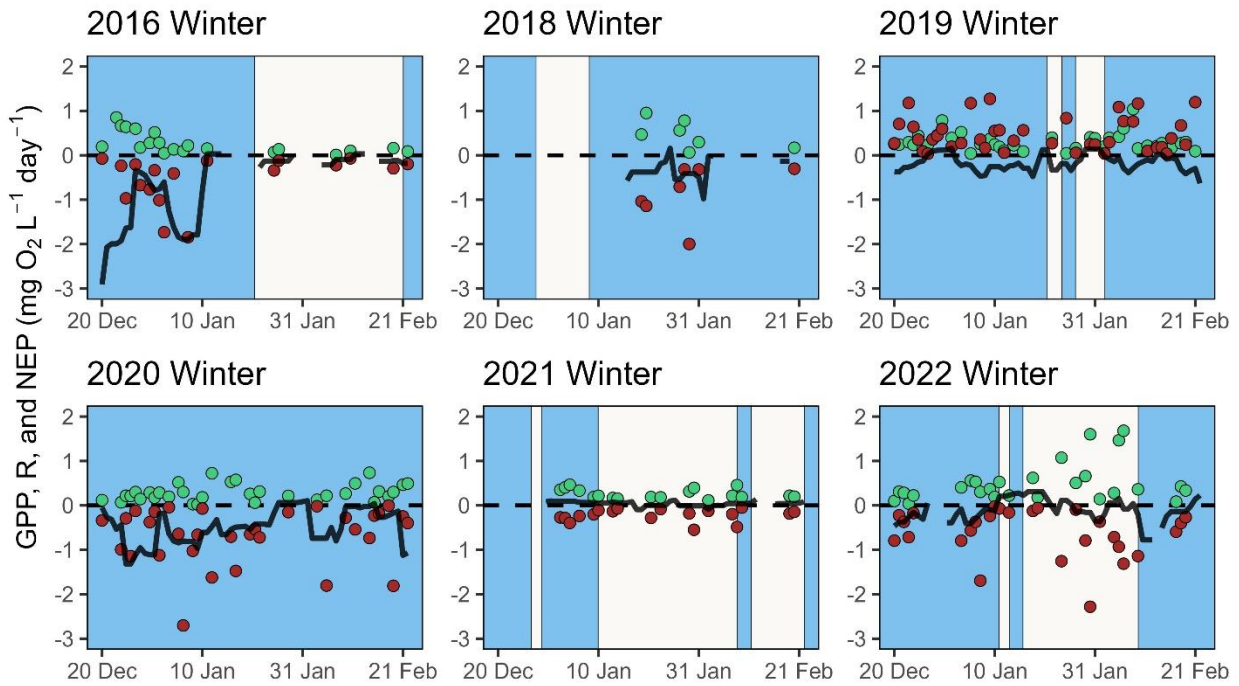
453

454

FCR experienced intermittent ice cover in most years, with up to three separate periods
 of ice cover within a winter season. Ice cover duration ranged from 0 days (2020) to 35 days of

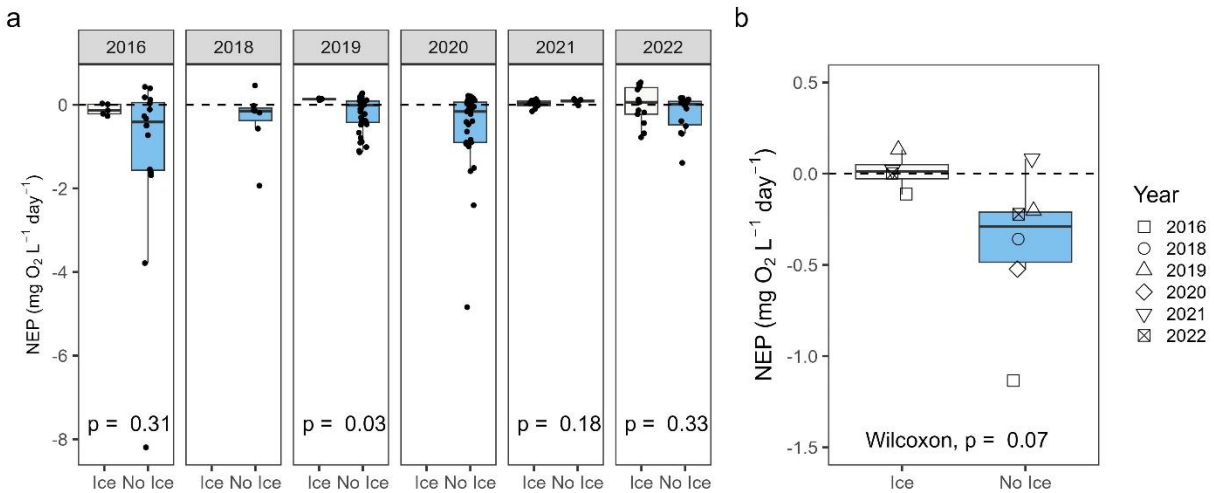
455 ice (2016) across the six winters (Figure 1b). In 2017 and 2021, FCR exhibited three separate
456 periods of ice cover throughout each winter, and in 2019 and 2022, two separate periods of ice
457 cover occurred. In contrast, there was only one period of continuous ice cover in 2016 and 2018
458 (Figure 1b).

459 Patterns of winter GPP, R, and NEP were variable among years and durations of ice
460 cover (Figure 4). Overall, the inclusion of winter NEP estimates did not have a statistically
461 significant effect on annual NEP rates ($t_4 = -0.1$, $p = 0.93$; Figure 2b). Aggregated across all ice-
462 covered and ice-free winter periods, NEP was not statistically different in any year except for in
463 2019, when NEP was higher on ice-covered days than ice-free days in the winter (Figure 5a).
464 NEP was additionally not significantly different between ice-covered and ice-free days when
465 aggregated across years, though rates were slightly higher under-ice (Wilcoxon test $p = 0.07$;
466 Figure 5b). R was only significantly different between ice-covered and ice-free days in winter
467 2016 (lower under ice; Wilcoxon test $p = 0.03$). GPP was significantly different in 2016 and
468 2022, but the direction of effect differed between the two years (higher under ice in 2022, lower
469 in 2016; Wilcoxon test $p < 0.05$, Supplementary Figure S6).



470
471
472
473
474

Figure 4. Daily estimates of GPP (green points), R (brown points), and seven-day rolling average of NEP (black line) in different winter seasons. Blue-shaded rectangles denote open-water periods and white rectangles denote periods of ice cover. Metabolism estimates are excluded for winter 2017 due to missing DO data.



475

476 Figure 5. a) Boxplots of daily NEP rates for each winter season comparing days with ice cover
477 (white) and days without ice cover (blue). b) Boxplots comparing ice-covered and ice-free
478 median daily NEP estimates per year. There were no winter NEP estimates in 2018 on days
479 with ice cover, and winter 2020 had no days of ice cover.

480

481

482 3.3 Q3: *What are the most important drivers of variability in metabolism?*

483 Water chemistry variables were consistently important drivers of daily GPP (Table 2), but
484 there were no statistically significant models with environmental predictors of R or NEP. NEP
485 was more strongly correlated to R (Spearman rho = 0.58, $p < 0.001$) than GPP (Spearman rho =
486 0.21, $p < 0.001$). The model fits varied across the metabolism metrics, with substantially more
487 variation explained by our candidate environmental predictors for GPP ($R^2 = 0.55-0.57$), vs. R
488 and NEP ($R^2 = 0$; Table 2).

489 The top models predicting GPP had multiple environmental drivers (TN, SRP,
490 ammonium, Precipitation, and \bar{E}_{24}), which were all included in more than one best-fitting model
491 (Table 2). TN, SRP, and \bar{E}_{24} were positively associated with GPP in all of these models, and
492 ammonium and precipitation were negatively associated with GPP. Neither R or NEP had best-
493 fitting models with environmental drivers, as the top model for both metabolism metrics only
494 included the autoregressive lag term and had R^2 values of 0 (Table 2). We additionally tested
495 the effects of water temperature on metabolism rates, but the inclusion of water temperature did
496 not significantly alter our results in Table 2 (Supplementary Table S3).

497

Table 2. Best-fitting (within 2 AICc units of the top model), statistically significant autoregressive models for daily GPP, R, and NEP, listed in descending order. There were no statistically significant models for R and NEP, but we retained the base autoregressive models in the table for comparison. We tested the effects of seven candidate environmental drivers, which were z-transformed prior to analysis. GPP_{t-1} , NEP_{t-1} , and R_{t-1} are the one-day autoregressive lag terms in each metabolism model. The environmental drivers were: DOC = dissolved organic carbon, \bar{E}_{24} = mean light experienced by phytoplankton, NH_4 = ammonium, NO_3 = nitrate, Precip = total daily precipitation, SRP = soluble reactive phosphorus, TN = total nitrogen, and TP = total phosphorus.

| Model | Equation | AICc | R ² | p |
|-------|---|-------|----------------|---------|
| GPP | $GPP = 0.29(GPP_{t-1}) + 0.52(TN) + 0.23(\bar{E}_{24}) + 1.00$ | 114.7 | 0.55 | < 0.001 |
| | $GPP = 0.28(GPP_{t-1}) + 0.50(TN) + 0.22(\bar{E}_{24}) + 0.10(SRP) + 1.02$ | 114.8 | 0.56 | < 0.001 |
| | $GPP = 0.28(GPP_{t-1}) + 0.52(TN) + 0.21(\bar{E}_{24}) - 0.16(NH_4) + 0.12(SRP) + 1.01$ | 115.9 | 0.57 | < 0.001 |
| | $GPP = 0.30(GPP_{t-1}) + 0.53(TN) + 0.22(\bar{E}_{24}) - 0.11(NH_4) + 1$ | 116.4 | 0.55 | < 0.001 |
| | $GPP = 0.27(GPP_{t-1}) + 0.52(TN) + 0.21(\bar{E}_{24}) + 0.11(SRP) - 0.07(Precip) + 1.03$ | 116.4 | 0.57 | < 0.001 |
| | $GPP = 0.28(GPP_{t-1}) + 0.53(TN) + 0.23(\bar{E}_{24}) - 0.06(Precip) + 1.02$ | 116.5 | 0.55 | < 0.001 |
| R | $R = -0.02(R_{t-1}) - 1.5$ | 320.5 | 0.00 | 0.84 |
| NEP | $NEP = -0.04(NEP_{t-1}) - 0.23$ | 314.9 | 0.00 | 0.61 |

499 **4 Discussion**

500 We observed large variability in metabolism rates throughout six years in a small
501 eutrophic reservoir. While ice cover duration varied substantially between years, annual
502 metabolism estimates were similar between years (Figure 2c), and winter had similar rates of
503 NEP to other seasons (Figure 3). NEP was generally higher on ice-covered days than ice-free
504 days (Figure 5b), but this result was only statistically significant in winter 2019 (Figure 5a). GPP
505 and R, but not NEP, differed significantly between seasons (Figure 3), whereas NEP was the
506 only metabolism rate with significant inter-annual variation (Supplementary Figure S5). Water
507 chemistry parameters were a significant driver of GPP, while R and NEP were not significantly
508 predicted by any of the other candidate environmental drivers (Table 2). Below, we explore how
509 our results inform our understanding of intra- and inter-annual metabolism in a reservoir with
510 intermittent ice cover, as well as identify future directions for winter research.

511

512 *4.1 Under-ice metabolism rates compared to open-water metabolism*

513 Contrary to our hypotheses, the inclusion of winter did not significantly alter annual NEP
514 estimates (Figure 2c). Within the winter, ice-covered periods exhibited higher NEP than ice-free
515 periods in one year (2019), which had intermediate ice coverage relative to the other years
516 (Figure 4, Figure 5a), but it is possible that the duration of ice cover at FCR (0 to 35 days per
517 year) was overall too short to have a substantial effect on annual estimates in our six-year
518 study. Assuming that additional days of ice cover would exhibit the median NEP rates observed
519 under-ice in this study, a back-of-envelope calculation suggests that even an additional 100
520 days of ice per winter would not cause the inclusion of winter data to alter annual NEP
521 estimates (Supplementary Text S4, Table S4). Consequently, multiple months of ice cover per
522 winter may be needed for winter dynamics to significantly affect annual metabolism rates in our
523 study reservoir.

524 Similar NEP rates across seasons were contrary to our prediction that NEP would
525 decrease under ice, as observed in a previous study (Brentrup et al., 2021). We expected that
526 ice cover would lead to decreased primary production, resulting in greater R than GPP (Huang
527 et al., 2021; Obertegger et al., 2017). Instead, our results indicate the opposite pattern,
528 suggesting that ice-covered conditions promoted greater rates of primary production compared
529 to ice-free conditions in the winter (especially in Winter 2022; Figure 5). High concentrations of
530 phytoplankton under-ice have been observed in other studies (Leppäranta et al., 2012; Reinl et
531 al., 2023), in which phytoplankton can use the ice surface as a substrate, promoting growth that
532 may not otherwise occur in winter months (Twiss et al., 2012). Additionally, clear and thin ice
533 conditions may allow additional light penetration, leading to a more favorable environment for
534 phytoplankton growth under-ice (Leppäranta et al., 2012). FCR may be especially likely to
535 display clear ice conditions, as ice cover is often very short in the reservoir relative to north
536 temperate lakes (Weyhenmeyer et al., 2022), thus not providing enough time for ice layers to
537 become opaque as snow falls and freezes into ice or snowpack to accumulate on-ice.
538 Consequently, our study adds to the growing literature that suggests that ice cover can increase
539 GPP and NEP, not just R (Supplementary Figure S6).

540 Winter GPP and R estimates were significantly lower than in summer, but NEP was not
541 significantly different between the seasons (Figure 3). Higher GPP and R estimates in the
542 summer relative to winter have been observed in numerous studies (Hu et al., 2015; North et
543 al., 2023; Rabaey et al., 2021), but similar rates of NEP among seasons are less common (Hu
544 et al., 2015). Multiple studies have shown that NEP can shift from autotrophic in the summer to
545 heterotrophic in the winter, with shoulder seasons (i.e., the spring and fall) showing intermediary
546 rates between summer and winter (Brentrup et al., 2021; Rabaey et al., 2021). We note that
547 these previous studies were conducted in higher-latitude glacially-formed lakes that experience
548 multiple months of continuous ice cover (Brentrup et al., 2021; Rabaey et al., 2021). The
549 intermittent ice observed at FCR provides a unique comparison to these systems, as we do not

550 observe significant changes in NEP from summer to winter, possibly because the shorter ice
551 cover duration allows for an extended period of high light conditions relative to opaque ice, in
552 turn extending the phytoplankton growing period (Wetz et al., 2004).

553

554 *4.2 Inter and intra-annual variability in lake metabolism*

555 To the best of our knowledge, only two other studies have quantified metabolism rates in
556 lentic waterbodies for durations longer than one continuous year (Hu et al., 2015; Rabaey et al.,
557 2021). In these studies (Hu et al., 2015; Rabaey et al., 2021), both conducted in naturally-
558 formed lakes, the highest rates of GPP and R were observed in the summer and the lowest
559 rates were observed in the winter, similar to our findings. Hu et al. (2015) also found that
560 metabolism rates were more variable within a year across days than among years, while
561 Rabaey et al. (2021) did not compare inter-annual variation in metabolism rates.

562 Contrary to expectation, we did not observe a shift in NEP across seasons. Unlike
563 previous studies in which NEP shifted from positive to negative between summer and winter
564 (Rabaey et al. 2021), leading to changes in annual metabolism estimates (Brentrup et al. 2021),
565 FCR exhibited similar NEP year-round (Figure 3c). This consistency across seasons may be
566 potentially due to FCR's short ice cover duration or because it is a human-made reservoir and
567 therefore may exhibit fundamentally different patterns of ecosystem functioning than the
568 naturally-formed lakes examined by Brentrup et al. (2021) and Rabaey et al. (2021).

569 The prevalence of heterotrophy in reservoirs has been found to vary both over space
570 and time, with previous studies largely focusing on summer or ice-free periods (Barbosa et al.,
571 2023; Solomon et al., 2013; Williamson et al., 2021). Reservoirs have exhibited both net
572 heterotrophy (Barbosa et al., 2023; Solomon et al., 2013) and autotrophy (Solomon et al.,
573 2013), with some studies showing changes between years (Williamson et al., 2021). We
574 observed small shifts from autotrophy to heterotrophy in the winter (Figure 4), in addition to
575 other seasons (Figure 2b), which has also been observed in previous reservoir studies (Barbosa

576 et al., 2023; Williamson et al., 2021). Throughout the year, we observed mostly heterotrophic
577 conditions, which was consistent with three large oligotrophic reservoirs in Canada (Barbosa et
578 al., 2023). It is possible that FCR consistently exhibited net heterotrophy because of its short
579 residence time and continuous loading of allochthonous carbon (Park et al., 2009), motivating
580 the collection of organic carbon quality data in future studies to test this hypothesis.

581

582 *4.3 Water chemistry is an important driver of GPP*

583 This study is one of the first to explore the role of water chemistry (C, N, and P
584 concentrations) as drivers of variation in metabolism rates within a reservoir over time, as
585 several previous studies focused on the role of chemistry across lakes (e.g., Hanson et al.,
586 2003; Solomon et al., 2013) or only included meteorological and physical drivers (e.g., Brentrup
587 et al., 2021, Richardson et al., 2017). Nutrients were important drivers of GPP, with TN
588 appearing in all of the best-fitting AR models, and SRP appearing in half (Table 2). The
589 consistent appearance of TN and SRP in the list of best-fitting models predicting GPP support
590 co-limitation of phytoplankton growth in FCR, which has been previously observed in the
591 reservoir (Hamre et al., 2017), as well as numerous other freshwater ecosystems (e.g., Elser et
592 al., 2007; Lewis et al., 2020; Paerl et al., 2016; Volponi et al., 2023). The importance of TN
593 (instead of nitrate or ammonium) also highlights the potential role of organic N in FCR, which
594 has been found to stimulate phytoplankton growth more than inorganic N forms (Volponi et al.,
595 2023). We observed that ammonium was negatively correlated with GPP, which contradicts
596 previous work showing that ammonium is the preferred N form for phytoplankton uptake (Raven
597 et al., 1992). Despite this unexpected relationship, other studies have found that high
598 concentrations of ammonium can suppress algal growth rates (Glibert et al., 2016), and can
599 lead to decreases in N-fixing cyanobacteria (Yang et al., 2023), which often dominate FCR's
600 phytoplankton community in summer months (Lofton et al., 2022). Light was additionally found
601 to be a driver of GPP (Table 2), which was consistent with previous studies (Hu et al., 2015;

602 North et al., 2023), and highlights the important role ice may play altering GPP rates in FCR
603 (Leppäranta et al., 2012).

604 There were no significant environmental drivers of R or NEP in our AR models (Table 2),
605 which contradicted our expectation that inflow discharge or DOC would be a strong driver of R.
606 Previous studies have shown that DOC is often positively correlated with R and is an important
607 driver across lakes (Barbosa et al., 2023; Hanson et al., 2003; Solomon et al., 2013), but DOC
608 did not appear in top models for R (Table 2). It is possible that our candidate environmental
609 predictors did not include the most important drivers of R or NEP in FCR. For example, we did
610 not include wind speed as a potential environmental driver because it was an input to the
611 metabolism model to calculate k_t (eqn. 3) or organic matter quality due to lack of data; both of
612 these drivers have been found to be important in other freshwater ecosystems (Brentrup et al.,
613 2021; Jane & Rose, 2018). We found the inclusion of water temperature (another input to the
614 metabolism model) as an environmental predictor did not alter our results (Supplementary Table
615 S3), which was unexpected given previous work showing the importance of water temperature
616 on R (Yvon-Durocher et al., 2012), suggesting that the environmental drivers of metabolism in
617 FCR are complex and that monitoring of additional environmental variables is likely needed to
618 improve our understanding of its metabolism.

619 In addition to expanding environmental drivers of metabolism in future work, our study's
620 limitations motivate further follow-up analyses. First, our work underscores the importance of
621 monitoring metabolism in additional reservoirs across years. Our study was limited by changes
622 in DO and temperature sensors through the study, but differences in metabolism between years
623 with different dissolved oxygen and temperature sensors were minimal (Figure 3). While we
624 were only able to explore the effects of ice cover on metabolism in one reservoir, year-round
625 monitoring and long-term ice cover records for additional lakes and reservoirs is needed to
626 improve our understanding of how winter conditions affect ecosystem function across a gradient
627 of freshwater ecosystems. Second, in our analysis of the effects of winter ice cover on

628 metabolism, we were limited by the longest ice duration observed during our study period (35
629 days in 2016), which was two to four months shorter than previous winter metabolism studies
630 (Brentrup et al. 2021; Obertegger et al., 2017). Given the shorter ice cover duration in FCR, our
631 results are inherently different from prior ice-cover studies that experienced deep snowpack on
632 the ice that altered light penetration and GPP rates (Leppäranta et al., 2012; North et al., 2023).
633 Third, our monitoring data did not include records for ice thickness or transparency, which would
634 have improved understanding of the underwater light environment in the winter and subsequent
635 effects on GPP rates (Leppäranta et al., 2012), but were logistically impossible to collect due to
636 the danger of sampling intermittent ice conditions. Future work studying under-ice metabolism
637 would benefit from including under-ice light measurements, when feasible.

638

639 *4.4 What is winter and its role in ecosystem function?*

640 In this study, we classify seasons using operational definitions to understand how
641 intermittent ice cover is affecting lake metabolism. Many previous winter limnology studies have
642 either classified seasons based on presence/absence of thermal stratification or solar seasons
643 classifications (equinox and solstices; Ladwig et al., 2021; Rabaey et al., 2021). Assessing
644 thermal structure and density gradients from surface to sediments in a waterbody allows
645 determination of classical limnological periods in dimictic waterbodies, which include summer
646 stratification, spring and fall mixis, and winter inverse stratification under-ice (Gray et al., 2020;
647 Pierson et al., 2011; Woolway et al., 2022). However, this classification is not suited for
648 waterbodies with intermittent ice and inverse stratification, as seasons cannot be easily
649 delineated if “winter” starts and stops multiple times. The difficulty of using thermal stratification
650 to delineate seasons because of intermittent ice led to our operational definition of winter, in
651 which we defined winter as the duration of the earliest day of ice cover recorded in our study
652 time period (20 December) to the latest day of ice cover recorded in our study period (22
653 February). This classification led us to adjust our classification of a lake-year to start on 20

654 December, similar to how hydrologic studies use the water year (start date of 1 October) to
655 account for snowpack formation (Granato et al., 2017). With a consistent winter season across
656 years, we were also able to compare the impacts of different ice cover durations on not only
657 annual metabolism rates (Figure 2b), but within seasons as well (Figure 5). We note that
658 multiple other delineations of seasons (thermal stratification, solar calendars) yielded
659 qualitatively similar metabolism comparisons across seasons (Supplementary Text S3, Figure
660 S4), supporting the use of our operational definition of seasons.

661 Decreases in ice cover and the increased prevalence of intermittent ice cover on
662 waterbodies accelerate the need to understand how changing winter is affecting freshwater
663 ecosystem functioning. FCR at 37 °N is a sentinel of future conditions for lakes located at higher
664 latitudes, which will continue to experience shorter ice cover durations and increases in
665 intermittency (Sharma et al., 2019). Decreasing ice cover is especially important given our
666 contrasting findings to previous winter metabolism studies that found winter NEP to be more
667 heterotrophic than summer NEP (Brentrup et al., 2021; Rabaey et al., 2021). If higher latitude
668 lakes become more similar to FCR in the future, with more similar winter and summer NEP
669 dynamics, the role of lakes and reservoirs as carbon sources or sinks may change.

670

671 **5 Conclusions**

672 Our results provide useful insight into the role of intermittent ice cover on reservoir
673 ecosystem metabolism. We observed heterotrophic conditions across seasons, and no
674 significant influence of winter rates on annual metabolism rates, differing from previous studies
675 (e.g., Brentrup et al., 2021; Rabaey et al., 2021). We additionally found that water chemistry
676 was a consistent driver of variability in GPP. Our results may foreshadow future metabolism
677 dynamics in higher-latitude lakes and reservoirs as ice cover duration decreases and
678 intermittency increases. Altogether, our work highlights the need for year-round metabolism

679 studies spanning multiple years to both provide better estimates of seasonal and annual
680 metabolism, as well as establish baseline conditions as winter conditions continue to change.

681 682 **Acknowledgements**

683
684 We thank the Western Virginia Water Authority for access to our field site and their long-term
685 collaboration, which enabled this study. We thank B. Niederlehner, Heather Wander, and Mary
686 Lofton for assistance with chemical analyses of samples. The Virginia Tech Reservoir Group
687 provided helpful feedback on this manuscript. This work was financially supported by NSF DEB-
688 1753639, DBI-1933016, EF-2318661, DEB-2327030, and the VA Water Resources Research
689 Center. ASL acknowledges support for her Ph.D. from the Virginia Tech College of Science
690 Roundtable, the Institute for Critical Technology and Applied Science (ICTAS), and a NSF
691 Graduate Research Fellowship (GRFP; DGE-1840995).

692 693 **Open Research**

694 All data used in this analysis are published in the Environmental Data Initiative (EDI) repository
695 and cited throughout the manuscript: Carey & Breef-Pilz (2022); Carey & Breef-Pilz (2023a);
696 Carey & Breef-Pilz (2023b); Carey, Lewis, et al., (2022); Carey, Breef-Pilz, Wander, et al.,
697 (2023); Carey, Lewis, & Breef-Pilz (2023); Carey, Breef-Pilz, & Woelmer (2023); Carey, Howard,
698 Gantzer, et al., (2023); and Carey, Wander, Howard, et al., (2023). Code used to conduct this
699 analysis is published in a Zenodo repository (Howard et al., 2024).

700 701 702 **References**

- 703
704 Andersen, M. R., Sand-Jensen, K., Iestyn Woolway, R., & Jones, I. D. (2017). Profound daily
705 vertical stratification and mixing in a small, shallow, wind-exposed lake with submerged
706 macrophytes. *Aquatic Sciences*, 79(2), 395–406. [https://doi.org/10.1007/s00027-016-](https://doi.org/10.1007/s00027-016-0505-0)
707 0505-0
- 708 Barbosa, P. M., Bodmer, P., Stadler, M., Rust, F., Tremblay, A., & Del Giorgio, P. A. (2023).
709 Ecosystem Metabolism Is the Dominant Source of Carbon Dioxide in Three Young
710 Boreal Cascade-Reservoirs (La Romaine Complex, Québec). *Journal of Geophysical*
711 *Research: Biogeosciences*, 128(4), e2022JG007253.
712 <https://doi.org/10.1029/2022JG007253>
- 713 Bartoń, K. (2022). MuMIn: Multi-Model Inference. R package version 1.47.1,
714 <https://CRAN.R-project.org/package=MuMIn>
- 715 Block, B. D., Denfeld, B. A., Stockwell, J. D., Flaim, G., Grossart, H. F., Knoll, L. B., et al.
716 (2019). The unique methodological challenges of winter limnology. *Limnology and*
717 *Oceanography: Methods*, 17(1), 42–57. <https://doi.org/10.1002/lom3.10295>
- 718 Box, G. E. P., & Pierce, D. A. (1970). Distribution of Residual Autocorrelations in
719 Autoregressive-Integrated Moving Average Time Series. *Journal of American Statistical*
720 *Association*, 65(332), 1509–1526.
- 721 Brentrup, J. A., Richardson, D. C., Carey, C. C., Ward, N. K., Bruesewitz, D. A., & Weathers, K.
722 C. (2021). Under-ice respiration rates shift the annual carbon cycle in the mixed layer of

723 an oligotrophic lake from autotrophy to heterotrophy. *Inland Waters*, 11(1), 114–123.
724 <https://doi.org/10.1080/20442041.2020.1805261>

725 Carey, C. C., & Breef-Pilz, A. (2022). Ice cover data for Falling Creek Reservoir and Beaverdam
726 Reservoir, Vinton, Virginia, USA for 2013-2022 [Data set]. Environmental Data Initiative.
727 <https://doi.org/10.6073/PASTA/917B3947D91470EECF979E9297ED4D2E>

728 Carey, C. C., & Breef-Pilz, A. (2023a). Time series of high-frequency meteorological data at
729 Falling Creek Reservoir, Virginia, USA 2015-2022 [Data set]. Environmental Data
730 Initiative. <https://doi.org/10.6073/PASTA/F3F97C7FDD287C29084BF52FC759A801>

731 Carey, C. C., & Breef-Pilz, A. (2023b). Discharge time series for the primary inflow tributary
732 entering Falling Creek Reservoir, Vinton, Virginia, USA 2013-2022 [Data set].
733 Environmental Data Initiative.
734 <https://doi.org/10.6073/PASTA/791192BEF17F21E8C0641EA903440A16>

735 Carey, C. C., Hanson, P. C., Thomas, R. Q., Gerling, A. B., Hounshell, A. G., Lewis, A. S. L., et
736 al. (2022). Anoxia decreases the magnitude of the carbon, nitrogen, and phosphorus
737 sink in freshwaters. *Global Change Biology*, 28(16), 4861–4881.
738 <https://doi.org/10.1111/gcb.16228>

739 Carey, C. C., Lewis, A. S. L., Howard, D. W., Woelmer, W. M., Gantzer, P. A., Bierlein, K. A., et
740 al. (2022). Bathymetry and watershed area for Falling Creek Reservoir, Beaverdam
741 Reservoir, and Carvins Cove Reservoir [Data set]. Environmental Data Initiative.
742 <https://doi.org/10.6073/PASTA/352735344150F7E77D2BC18B69A22412>

743 Carey, C. C., Breef-Pilz, A., Wander, H. L., Geisler, B., & Haynie, G. (2023). Secchi depth data
744 and discrete depth profiles of water temperature, dissolved oxygen, conductivity, specific
745 conductance, photosynthetic active radiation, redox potential, and pH for Beaverdam
746 Reservoir, Carvins Cove Reservoir, Falling Creek Reservoir, Gatewood Reservoir, and
747 Spring Hollow Reservoir in southwestern Virginia, USA 2013-2022 [Data set].
748 Environmental Data Initiative.
749 <https://doi.org/10.6073/PASTA/EB17510D09E66EF79D7D54A18CA91D61>

750 Carey, C. C., Lewis, A. S. L., & Breef-Pilz, A. (2023). Time series of high-frequency profiles of
751 depth, temperature, dissolved oxygen, conductivity, specific conductance, chlorophyll a,
752 turbidity, pH, oxidation-reduction potential, photosynthetic active radiation, and descent
753 rate for Beaverdam Reservoir, Carvins Cove Reservoir, Falling Creek Reservoir,
754 Gatewood Reservoir, and Spring Hollow Reservoir in southwestern Virginia, USA 2013-
755 2022 [Data set]. Environmental Data Initiative.
756 <https://doi.org/10.6073/PASTA/5170B52F7514F54D834130DB0EFC5565>

757 Carey, C. C., Breef-Pilz, A., & Woelmer, W. M. (2023). Time series of high-frequency sensor
758 data measuring water temperature, dissolved oxygen, pressure, conductivity, specific
759 conductance, total dissolved solids, chlorophyll a, phycocyanin, fluorescent dissolved
760 organic matter, and turbidity at discrete depths in Falling Creek Reservoir, Virginia, USA
761 in 2018-2022 [Data set]. Environmental Data Initiative.
762 <https://doi.org/10.6073/PASTA/F6BB4F5F602060DEC6652FF8EB555082>

763 Carey, C. C., Howard, D. W., Gantzer, P. A., McClure, R. P., Gerling, A. B., Lofton, M. E., et al.
764 (2023). Time series of high-frequency sensors measuring water temperature and
765 dissolved oxygen at discrete depths in Falling Creek Reservoir, Virginia, USA in 2012-

766 2018 [Data set]. Environmental Data Initiative.
767 <https://doi.org/10.6073/PASTA/964A5BBBB4D5826B5ACB30098DBAE59A>
768 Carey, C. C., Wander, H. L., Howard, D. W., Breef-Pilz, A., & Niederlehner, B. R. (2023). Water
769 chemistry time series for Beaverdam Reservoir, Carvins Cove Reservoir, Falling Creek
770 Reservoir, Gatewood Reservoir, and Spring Hollow Reservoir in southwestern Virginia,
771 USA 2013-2022 [Data set]. Environmental Data Initiative.
772 <https://doi.org/10.6073/PASTA/457120A9DE886A1470C22A01D808AB2D>
773 Catalán, N., Marcé, R., Kothawala, D. N., & Tranvik, Lars. J. (2016). Organic carbon
774 decomposition rates controlled by water retention time across inland waters. *Nature*
775 *Geoscience*, 9, 501–504. <https://doi.org/10.1038/ngeo2720>
776 Cole, J. J., & Caraco, N. F. (1998). Atmospheric exchange of carbon dioxide in a low-wind
777 oligotrophic lake measured by the addition of SF 6. *Limnology and Oceanography*,
778 43(4), 647–656. <https://doi.org/10.4319/lo.1998.43.4.0647>
779 Coloso, J. J., Cole, J. J., & Pace, M. L. (2011). Difficulty in Discerning Drivers of Lake
780 Ecosystem Metabolism with High-Frequency Data. *Ecosystems*, 14(6), 935–948.
781 <https://doi.org/10.1007/s10021-011-9455-5>
782 Doubek, J. P., & Carey, C. C. (2017). Catchment, morphometric, and water quality
783 characteristics differ between reservoirs and naturally formed lakes on a latitudinal
784 gradient in the conterminous United States. *Inland Waters*, 7(2), 171–180.
785 <https://doi.org/10.1080/20442041.2017.1293317>
786 Duka, M. A., Shintani, T., & Yokoyama, K. (2021). Thermal stratification responses of a
787 monomictic reservoir under different seasons and operation schemes. *Science of The*
788 *Total Environment*, 767, 144423. <https://doi.org/10.1016/j.scitotenv.2020.144423>
789 Elser, J. J., Bracken, M. E. S., Cleland, E. E., Gruner, D. S., Harpole, W. S., Hillebrand, H., et al.
790 (2007). Global analysis of nitrogen and phosphorus limitation of primary producers in
791 freshwater, marine and terrestrial ecosystems. *Ecology Letters*, 10(12), 1135–1142.
792 <https://doi.org/10.1111/j.1461-0248.2007.01113.x>
793 Fox, J., & Weisberg, S. (2019). *An {R} Companion to Applied Regression*, Third Edition.
794 Thousand Oaks CA: Sage. URL:
795 <https://socialsciences.mcmaster.ca/jfox/Books/Companion/>
796 Gerling, A. B., Browne, R. G., Gantzer, P. A., Mobley, M. H., Little, J. C., & Carey, C. C. (2014).
797 First report of the successful operation of a side stream supersaturation hypolimnetic
798 oxygenation system in a eutrophic, shallow reservoir. *Water Research*, 67, 129–143.
799 <https://doi.org/10.1016/j.watres.2014.09.002>
800 Gerling, A. B., Munger, Z. W., Doubek, J. P., Hamre, K. D., Gantzer, P. A., Little, J. C., & Carey,
801 C. C. (2016). Whole-Catchment Manipulations of Internal and External Loading Reveal
802 the Sensitivity of a Century-Old Reservoir to Hypoxia. *Ecosystems*, 19(3), 555–571.
803 <https://doi.org/10.1007/s10021-015-9951-0>
804 Glibert, P. M., Wilkerson, F. P., Dugdale, R. C., Raven, J. A., Dupont, C. L., Leavitt, P. R., et al.
805 (2016). Pluses and minuses of ammonium and nitrate uptake and assimilation by
806 phytoplankton and implications for productivity and community composition, with
807 emphasis on nitrogen-enriched conditions: Pluses and minuses of NH₄⁺ and NO₃⁻.
808 *Limnology and Oceanography*, 61(1), 165–197. <https://doi.org/10.1002/lno.10203>

809 Granato, G. E., Ries III, K. G., & Steeves, P. A. (2017). Compilation of streamflow statistics
810 calculated from daily mean streamflow data collected during water years 1901–2015 for
811 selected U.S. Geological Survey streamgages. U.S. Geological Survey Open-File Report
812 2017–1108. <https://doi.org/10.3133/ofr20171108>

813 Gray, E., Mackay, E. B., Elliott, J. A., Folkard, A. M., & Jones, I. D. (2020). Wide-spread
814 inconsistency in estimation of lake mixed depth impacts interpretation of limnological
815 processes. *Water Research*, 168, 115136. <https://doi.org/10.1016/j.watres.2019.115136>

816 Guildford, S. J., Bootsma, H. A., Fee, E. J., Hecky, R. E., & Patterson, G. (2000). Phytoplankton
817 nutrient status and mean water column irradiance in Lakes Malawi and Superior. *Aquatic*
818 *Ecosystem Health & Management*, 3(1), 35–45.
819 <https://doi.org/10.1080/14634980008656989>

820 Hampton, S. E., Galloway, A. W. E., Powers, S. M., Ozersky, T., Woo, K. H., Batt, R. D., et al.
821 (2017). Ecology under lake ice. *Ecology Letters*, 20, 98–111.
822 <https://doi.org/10.1111/ele.12699>

823 Hamre, K. D., Gerling, A. B., Munger, Z. W., Doubek, J. P., McClure, R. P., Cottingham, K. L., &
824 Carey, C. C. (2017). Spatial variation in dinoflagellate recruitment along a reservoir
825 ecosystem continuum. *Journal of Plankton Research*, 39(4), 715–728.
826 <https://doi.org/10.1093/plankt/fbx004>

827 Hanson, P. C., Bade, D. L., Carpenter, S. R., & Kratz, T. K. (2003). Lake metabolism:
828 Relationships with dissolved organic carbon and phosphorus. *Limnology and*
829 *Oceanography*, 48(3), 1112–1119. <https://doi.org/10.4319/lo.2003.48.3.1112>

830 Hanson, P. C., Carpenter, S. R., Kimura, N., Wu, C., Cornelius, S. P., & Kratz, T. K. (2008).
831 Evaluation of metabolism models for free-water dissolved oxygen methods in lakes.
832 *Limnology and Oceanography: Methods*, 6, 454–465.
833 <https://doi.org/10.4319/lom.2008.6.454>

834 Hayes, N. M., Deemer, B. R., Corman, J. R., Razavi, N. R., & Strock, K. E. (2017). Key
835 differences between lakes and reservoirs modify climate signals: A case for a new
836 conceptual model. *Limnology and Oceanography Letters*, 2(2), 47–62.
837 <https://doi.org/10.1002/lo2.10036>

838 Hoellein, T. J., Bruesewitz, D. A., & Richardson, D. C. (2013). Revisiting Odum (1956): A
839 synthesis of aquatic ecosystem metabolism. *Limnology and Oceanography*, 58(6),
840 2089–2100. <https://doi.org/10.4319/lo.2013.58.6.2089>

841 Hollander, M., & Wolfe, D.A. (1973). *Nonparametric Statistical Methods*. New York: John Wiley
842 & Sons. Pages 115–120.

843 Howard, D. W., Hounshell, A. G., Lofton, M. E., Woelmer, W. M., Hanson, P. C., & Carey, C. C.
844 (2021). Variability in fluorescent dissolved organic matter concentrations across diel to
845 seasonal time scales is driven by water temperature and meteorology in a eutrophic
846 reservoir. *Aquatic Sciences*, 83(30). <https://doi.org/10.1007/s00027-021-00784-w>

847 Howard, D., Brentrup, J., Richardson, D., Lewis, A., Olsson, F., & Carey, C. (2024).
848 *dwh77/FCR_Metab: Metabolism estimates in Falling Creek Reservoir (v1.0)*. Zenodo.
849 <https://doi.org/10.5281/zenodo.10575646>

850 Hu, Z., Xiao, Q., Yang, J., Xiao, W., Wang, W., Liu, S., & Lee, X. (2015). Temporal Dynamics
851 and Drivers of Ecosystem Metabolism in a Large Subtropical Shallow Lake (Lake Taihu).

852 International Journal of Environmental Research and Public Health, 12(4), 3691–3706.
853 <https://doi.org/10.3390/ijerph120403691>

854 Huang, W., Zhang, Z., Li, Z., Leppäranta, M., Arvola, L., Song, S., et al. (2021). Under-ice
855 dissolved oxygen and metabolism dynamics in a shallow lake: The critical role of ice and
856 snow. *Water Resources Research*, 57, e2020WR027990.
857 <https://doi.org/10.1029/2020wr027990>

858 Idso, S. B. (1973). On the concept of lake stability. *Limnology and Oceanography*, 18(4), 681–
859 683. <https://doi.org/10.4319/lo.1973.18.4.0681>

860 IPCC (2022). *Climate Change 2022: Impacts, Adaptation, and Vulnerability. Contribution of*
861 *Working Group II to the Sixth Assessment Report of the Intergovernmental Panel on*
862 *Climate Change* [H.-O. Pörtner, D.C. Roberts, M. Tignor, E.S. Poloczanska, K.
863 Mintenbeck, A. Alegría, M. Craig, S. Langsdorf, S. Löschke, V. Möller, A. Okem, B.
864 Rama (eds.)]. Cambridge University Press. Cambridge University Press, Cambridge, UK
865 and New York, NY, USA, 3056 pp., <https://doi.org/10.1017/9781009325844>.

866 Jane, S. F., & Rose, K. C. (2018). Carbon quality regulates the temperature dependence of
867 aquatic ecosystem respiration. *Freshwater Biology*, 63(11), 1407–1419.
868 <https://doi.org/10.1111/fwb.13168>

869 Jane, S. F., Mincer, J. L., Lau, M. P., Lewis, A. S. L., Stetler, J. T., & Rose, K. C. (2023). Longer
870 duration of seasonal stratification contributes to widespread increases in lake hypoxia
871 and anoxia. *Global Change Biology*, 29(4), 1009–1023.
872 <https://doi.org/10.1111/gcb.16525>

873 Jewson, D. H., Granin, N. G., Zhdanov, A. A., & Gnatovsky, R. Y. (2009). Effect of snow depth
874 on under-ice irradiance and growth of *Aulacoseira baicalensis* in Lake Baikal. *Aquatic*
875 *Ecology*, 43(3), 673–679. <https://doi.org/10.1007/s10452-009-9267-2>

876 Klug, J. L., Richardson, D. C., Ewing, H. A., Hargreaves, B. R., Samal, N. R., Vachon, D., et al.
877 (2012). Ecosystem effects of a tropical cyclone on a network of lakes in northeastern
878 North America. *Environmental Science and Technology*, 46(21), 11693–11701.
879 <https://doi.org/10.1021/es302063v>

880 Ladwig, R., Hanson, P. C., Dugan, H. A., Carey, C. C., Zhang, Y., Shu, L., et al. (2021). Lake
881 thermal structure drives interannual variability in summer anoxia dynamics in a eutrophic
882 lake over 37 years. *Hydrology and Earth System Sciences*, 25(2), 1009–1032.
883 <https://doi.org/10.5194/hess-25-1009-2021>

884 Ladwig, R., Appling, A. P., Delany, A., Dugan, H. A., Gao, Q., Lottig, N., et al. (2022). Long-term
885 change in metabolism phenology in north temperate lakes. *Limnology and*
886 *Oceanography*, 67(7), 1502–1521. <https://doi.org/10.1002/lno.12098>

887 Leppäranta, M., Heini, A., Jaatinen, E., & Arvola, L. (2012). The influence of ice season on the
888 physical and ecological conditions in Lake Vanajanselkä, southern Finland. *Water*
889 *Quality Research Journal*, 47(3–4), 287–299. <https://doi.org/10.2166/wqrj.2012.003>

890 Lewis, A. S. L., Kim, B. S., Edwards, H. L., Wander, H. L., Garfield, C. M., Murphy, H. E., et al.
891 (2020). Prevalence of phytoplankton limitation by both nitrogen and phosphorus related
892 to nutrient stoichiometry, land use, and primary producer biomass across the
893 northeastern United States. *Inland Waters*, 10(1), 42–50.
894 <https://doi.org/10.1080/20442041.2019.1664233>

895 Lofton, M. E., Howard, D. W., McClure, R. P., Wander, H. L., Woelmer, W. M., Hounshell, A. G.,
896 et al. (2022). Experimental thermocline deepening alters vertical distribution and
897 community structure of phytoplankton in a 4-year whole-reservoir manipulation.
898 *Freshwater Biology*, 67(11), 1903–1924. <https://doi.org/10.1111/fwb.13983>

899 Lovett, G. M., Cole, J. J., & Pace, M. L. (2006). Is Net Ecosystem Production Equal to
900 Ecosystem Carbon Accumulation? *Ecosystems*, 9(1), 152–155.
901 <https://doi.org/10.1007/s10021-005-0036-3>

902 Magnuson, J. J., Robertson, D. M., Benson, B. J., Wynne, R. H., Livingstone, D. M., Arai, T., et
903 al. (2000). Historical trends in lake and river ice cover in the Northern Hemisphere.
904 *Science*, 289(5485), 1743–1746. <https://doi.org/10.1126/science.289.5485.1743>

905 McClure, R. P., Lofton, M. E., Chen, S., Krueger, K. M., Little, J. C., & Carey, C. C. (2020). The
906 magnitude and drivers of methane ebullition and diffusion vary on a longitudinal gradient
907 in a small freshwater reservoir. *Journal of Geophysical Research: Biogeosciences*, 125,
908 e2019JG005205. <https://doi.org/10.1029/2019jg005205>

909 North, R., Venkiteswaran, J., Silsbe, G., Harrison, J., Hudson, J., Smith, R., et al. (2023). Winter
910 matters: year-round metabolism in temperate water bodies. *EarthArXiv*.
911 <https://doi.org/10.31223/X5RQ1V>

912 Obertegger, U., Obrador, B., & Flaim, G. (2017). Dissolved oxygen dynamics under ice: Three
913 winters of high-frequency data from Lake Tovel, Italy. *Water Resources Research*, 53,
914 7234–7246. <https://doi.org/10.1002/2017WR020599>

915 Odum, H. T. (1956). Primary Production in Flowing Waters. *Limnology and Oceanography*, 1(2),
916 102–117. <https://doi.org/10.4319/lo.1956.1.2.0102>

917 Ogle D.H., Doll J.C., Wheeler A.P., Dinno A. (2023). FSA: Simple Fisheries Stock Assessment
918 Methods. R package version 0.9.5, <https://CRAN.R-project.org/package=FSA>

919 Oleksy, I. A., Jones, S. E., & Solomon, C. T. (2022). Hydrologic Setting Dictates the Sensitivity
920 of Ecosystem Metabolism to Climate Variability in Lakes. *Ecosystems*, 25(6), 1328–
921 1345. <https://doi.org/10.1007/s10021-021-00718-5>

922 Pace, M. L., Buelo, C. D., & Carpenter, S. R. (2021). Phytoplankton biomass, dissolved organic
923 matter, and temperature drive respiration in whole lake nutrient additions. *Limnology and
924 Oceanography*, 66, 2174–2186. <https://doi.org/10.1002/lno.11738>

925 Paerl, H. W., Scott, J. T., McCarthy, M. J., Newell, S. E., Gardner, W. S., Havens, K. E., et al.
926 (2016). It Takes Two to Tango: When and Where Dual Nutrient (N & P) Reductions Are
927 Needed to Protect Lakes and Downstream Ecosystems. *Environmental Science &
928 Technology*, 50(20), 10805–10813. <https://doi.org/10.1021/acs.est.6b02575>

929 Palmer, M. A., & Richardson, D. C. (2009). VI.8 Provisioning Services: A Focus on Fresh Water.
930 In S. A. Levin, S. R. Carpenter, H. C. J. Godfray, A. P. Kinzig, M. Loreau, J. B. Losos, et
931 al. (Eds.), *The Princeton Guide to Ecology* (pp. 625–633). Princeton University Press.
932 <https://doi.org/10.1515/9781400833023.625>

933 Park, H., Byeon, M., Shin, Y., & Jung, D. (2009). Sources and spatial and temporal
934 characteristics of organic carbon in two large reservoirs with contrasting hydrologic
935 characteristics. *Water Resources Research*, 45(11), 2009WR008043.
936 <https://doi.org/10.1029/2009WR008043>

937 Pernica, P., North, R. L., & Baulch, H. M. (2017). In the cold light of day: the potential
938 importance of under-ice convective mixed layers to primary producers. *Inland Waters*,
939 7(2), 138–150. <https://doi.org/10.1080/20442041.2017.1296627>

940 Pierson, D. C., Weyhenmeyer, G. A., Arvola, L., Benson, B., Blenckner, T., Kratz, T., et al.
941 (2011). An automated method to monitor lake ice phenology. *Limnology and*
942 *Oceanography: Methods*, 9(2), 74–83. <https://doi.org/10.4319/lom.2010.9.0074>

943 R Core Team (2023). R: A language and environment for statistical computing. R Foundation for
944 Statistical Computing, Vienna, Austria. URL <https://www.R-project.org/>.

945 Rabaey, J. S., Domine, L. M., Zimmer, K. D., & Cotner, J. B. (2021). Winter Oxygen Regimes in
946 Clear and Turbid Shallow Lakes. *Journal of Geophysical Research: Biogeosciences*,
947 126, e2020JG006065. <https://doi.org/10.1029/2020JG006065>

948 Raven, J. A., Wollenweber, B., & Handley, L. L. (1992). A comparison of ammonium and nitrate
949 as nitrogen sources for photolithotrophs. *New Phytologist*, 121(1), 19–32.
950 <https://doi.org/10.1111/j.1469-8137.1992.tb01088.x>

951 Reinl, K. L., Harris, T. D., North, R. L., Almela, P., Berger, S. A., Bizic, M., et al. (2023). Blooms
952 also like it cold. *Limnology and Oceanography Letters*, 8(4), 546–564.
953 <https://doi.org/10.1002/lo.10316>

954 Richardson, D. C., Carey, C. C., Bruesewitz, D. A., & Weathers, K. C. (2017). Intra- and inter-
955 annual variability in metabolism in an oligotrophic lake. *Aquatic Sciences*, 79(2), 319–
956 333. <https://doi.org/10.1007/s00027-016-0499-7>

957 Sahoo, G. B., Forrest, A. L., Schladow, S. G., Reuter, J. E., Coats, R., & Dettinger, M. (2016).
958 Climate change impacts on lake thermal dynamics and ecosystem vulnerabilities:
959 Climate change impacts. *Limnology and Oceanography*, 61(2), 496–507.
960 <https://doi.org/10.1002/lno.10228>

961 Sharma, S., Blagrove, K., Magnuson, J. J., O'Reilly, C. M., Oliver, S., Batt, R. D., et al. (2019).
962 Widespread loss of lake ice around the Northern Hemisphere in a warming world. *Nature*
963 *Climate Change*, 9, 227–231. <https://doi.org/10.1038/s41558-018-0393-5>

964 Sharma, S., Richardson, D. C., Woolway, R. I., Imrit, M. A., Bouffard, D., Blagrove, K., et al.
965 (2021). Loss of Ice Cover, Shifting Phenology, and More Extreme Events in Northern
966 Hemisphere Lakes. *Journal of Geophysical Research: Biogeosciences*, 126(10), 1–12.
967 <https://doi.org/10.1029/2021JG006348>

968 Solomon, C. T., Bruesewitz, D. A., Richardson, D. C., Rose, K. C., Van de Bogert, M. C.,
969 Hanson, P. C., et al. (2013). Ecosystem respiration: Drivers of daily variability and
970 background respiration in lakes around the globe. *Limnology and Oceanography*, 58(3),
971 849–866. <https://doi.org/10.4319/lo.2013.58.3.0849>

972 Song, S., Li, C., Shi, X., Zhao, S., Tian, W., Li, Z., et al. (2019). Under-ice metabolism in a
973 shallow lake in a cold and arid climate. *Freshwater Biology*, 64(10), 1710–1720.
974 <https://doi.org/10.1111/fwb.13363>

975 Twiss, M. R., McKay, R. M. L., Bourbonniere, R. A., Bullerjahn, G. S., Carrick, H. J., Smith, R.
976 E. H., et al. (2012). Diatoms abound in ice-covered Lake Erie: An investigation of
977 offshore winter limnology in Lake Erie over the period 2007 to 2010. *Journal of Great*
978 *Lakes Research*, 38(1), 18–30. <https://doi.org/10.1016/j.jglr.2011.12.008>

979 Van de Bogert, M. C., Carpenter, S. R., Cole, J. J., & Pace, M. L. (2007). Assessing pelagic and
980 benthic metabolism using free water measurements: Benthic and pelagic metabolism.

981 Limnology and Oceanography: Methods, 5(5), 145–155.
982 <https://doi.org/10.4319/lom.2007.5.145>

983 Volponi, S. N., Wander, H. L., Richardson, D. C., Williams, C. J., Bruesewitz, D. A., Arnott, S., et
984 al. (2023). Nutrient function over form: Organic and inorganic nitrogen additions have
985 similar effects on lake phytoplankton nutrient limitation. *Limnology and Oceanography*,
986 68(2), 307–321. <https://doi.org/10.1002/lno.12270>

987 Wetz, M., Wheeler, P., & Letelier, R. (2004). Light-induced growth of phytoplankton collected
988 during the winter from the benthic boundary layer off Oregon, USA. *Marine Ecology*
989 *Progress Series*, 280, 95–104. <https://doi.org/10.3354/meps280095>

990 Weyhenmeyer, G. A., Obertegger, U., Rudebeck, H., Jakobsson, E., Jansen, J., Zdrovennova,
991 G., et al. (2022). Towards critical white ice conditions in lakes under global warming.
992 *Nature Communications*, 13(1), 4974. <https://doi.org/10.1038/s41467-022-32633-1>

993 Williamson, T. J., Vanni, M. J., & Renwick, W. H. (2021). Spatial and Temporal Variability of
994 Nutrient Dynamics and Ecosystem Metabolism in a Hyper-eutrophic Reservoir Differ
995 Between a Wet and Dry Year. *Ecosystems*, 24, 68–88. [https://doi.org/10.1007/s10021-](https://doi.org/10.1007/s10021-020-00505-8)
996 [020-00505-8](https://doi.org/10.1007/s10021-020-00505-8)

997 Winslow, L. A., Zwart, J. A., Batt, R. D., Dugan, H. A., Woolway, R. I., Corman, J. R., et al.
998 (2016). LakeMetabolizer: an R package for estimating lake metabolism from free-water
999 oxygen using diverse statistical models. *Inland Waters*, 6(4), 622–636.
1000 <https://doi.org/10.1080/IW-6.4.883>

1001 Winslow, L., Read, J., Woolway, R., Brentrup, J., Leach, T., Zwart, J., Albers, S., & Collinge, D.
1002 (2019). rLakeAnalyzer: Lake Physics Tools. R package version 1.11.4.1.
1003 <https://CRAN.R-project.org/package=rLakeAnalyzer>

1004 Woolway, R. I., Sharma, S., Weyhenmeyer, G. A., Debolskiy, A., Golub, M., Mercado-Bettín, D.,
1005 et al. (2021). Phenological shifts in lake stratification under climate change. *Nature*
1006 *Communications*, 12(1), 2318. <https://doi.org/10.1038/s41467-021-22657-4>

1007 Woolway, R. I., Denfeld, B., Tan, Z., Jansen, J., Weyhenmeyer, G. A., & La Fuente, S. (2022).
1008 Winter inverse lake stratification under historic and future climate change. *Limnology and*
1009 *Oceanography Letters*, 7(4), 302–311. <https://doi.org/10.1002/lol2.10231>

1010 Xia, Y., Mitchell, K., Ek, M., Sheffield, J., Cosgrove, B., Wood, E., et al. (2012). Continental-
1011 scale water and energy flux analysis and validation for the North American Land Data
1012 Assimilation System project phase 2 (NLDAS-2): 1. Intercomparison and application of
1013 model products. *Journal of Geophysical Research: Atmospheres*, 117(D3),
1014 2011JD016048. <https://doi.org/10.1029/2011JD016048>

1015 Yang, N., Li, Z., Wu, Z., Liu, X., Zhang, Y., Sun, T., et al. (2023). Differential effects of nitrate
1016 and ammonium on the growth of algae and microcystin production by nitrogen-fixing
1017 *Nostoc* sp. and non-nitrogen-fixing *Microcystis aeruginosa*. *Water Science &*
1018 *Technology*, 88(1), 136–150. <https://doi.org/10.2166/wst.2023.205>

1019 Yvon-Durocher, G., Caffrey, J. M., Cescatti, A., Dossena, M., Giorgio, P. D., Gasol, J. M., et al.
1020 (2012). Reconciling the temperature dependence of respiration across timescales and
1021 ecosystem types. *Nature*, 487(7408), 472–476. <https://doi.org/10.1038/nature11205>
1022